Size-Controlled Nanoparticle Clusters of Narrow Size-Polydispersity Formed Using Multiple Particle Types Through Competitive Stabilizer Desorption to a Liquid– Liquid Interface

Eoin K. Fox, Fadwa El Haddassi, Jose Hierrezuelo, Tsedev Ninjbadgar, Jacek K. Stolarczyk, Jenny Merlin, and Dermot F. Brougham*

A novel colloidal approach is presented for preparing fully dispersed nano- particle (NP) assemblies (clusters) of narrow size-polydispersity over a wide range of sizes through irreversible depletion of stabilizing ligands onto a liquid–liquid interface. Unusually, the relative monodispersity of the assemblies continuously improves throughout the process. A detailed kinetics study into the assembly of iron oxide NP clusters shows that the assembly rate decreases with NP concentration, pinpointing the role of the interface in size focusing. A new protocol for identifying initial conditions that enable controlled assembly is described, which allows extension of the approach to multiple NP types, opening up a general route to colloidally processed mate- rials. The process uses cheap materials, it is reproducible, robust, and scale- able, and it allows for selection of both particle and cluster size. In the case of assemblies of magnetic iron oxide NPs, these advantages enable tuning of the magnetic properties of the assemblies for applications such as magnetically targetable MRI-trackable agents in biomedicine.

1. Introduction

The formation of nanoparticle (NP) assemblies (i.e., aggregates or clusters comprising multiple particles) from pre-existing stable NP dispersions offers the possibility of size control on both the particle and cluster length scales. This advantage can be used to engineer the emergence of new collective properties due to interactions between individual NPs at close proximity. For instance, in the case of magnetic iron oxide, or FeO, NPs it is known that the assemblies have potential for improving medical diagnosis,[1–3] and for targeted drug delivery through the application of external magnetic fields.[4] The collective magnetic properties of FeO NP clusters (NPCs) for these applications are determined by particle and cluster size.[5] However, the formation of monodisperse assemblies (of magnetic, fluorescent and semi-conductor NPs, and of combinations of these) by colloidal processing of NP dispersions is a significant technical challenge and a barrier to applications.

We recently classified the state-of-the-art in colloidal assembly,[6] according to the nature of the key step wherein the dispersion is destabilized leading to three general types: i) "*Tuning of solvent/ligand interactions*" either by direct solvent exchange, e.g., by gradual evaporation of the volatile solvent (usually in the presence of a block copolymer for water stabilization) as suggested by Grubbs[7] and adopted by many groups,[8,9] or by external control of the media, e.g., by desalting[10] or addition of antisolvent.[11] ii) "*Phase collapse*" by destabilization of water-in-oil, or more typically oil-in-water, microemulsions/ micelles.[12] In most examples, using these two approaches, expensive block co-polymers are required and the methods are very sensitive to the starting conditions, and hence are difficult to scale-up or reproduce. iii) "*Ligand removal*" approaches can involve full ligand exchange, e.g., of long chain fatty acid with charged inorganic species.[13] As a result it is difficult to produce stable monodisperse NPC suspensions, so the products are usually used for preparing nanostructured solids.

Alternatively, we have developed partial ligand displacement, by competitive stabilizer desorption (CSD), for preparation of stable suspensions of size-controlled magnetic FeO NPCs using only inexpensive starting materials,[14–17] so addressing some of these limitations.

In CSD, a silica substrate is placed in contact with an organic suspension of preformed fully dispersed ligand stabilized NPs. The substrate competes for the stabilizing ligand (without interacting with the NPs directly) gradually reducing NP sur- face coverage and hence reducing steric repulsion between the particles, which results in ongoing formation of clusters in suspension. When the conditions are well controlled the assembly is gradual, it proceeds over a period of hours and leads to monodisperse NPCs.[16] As a result, the process can be arrested at any time by either removal of the silica phase or by addition of excess ligand. In this way both the NP and the final NPC size can be selected for the application of interest and binary clusters can be formed.[14,15] More recently we exploited this unique advantage to prepare clusters of FeO NPs for which the collective magneto-crystalline anisotropy was determined only by the MNP size, enabling preparation of clusters of any desired size with selectable anisotropy.[17] However, it is difficult to avoid variability of the silica (powder) surface area between experiments, hence the process is not robust, or easily reproduced and so is difficult to scale-up. In addition the silica substrate is expensive and its properties vary between batches.

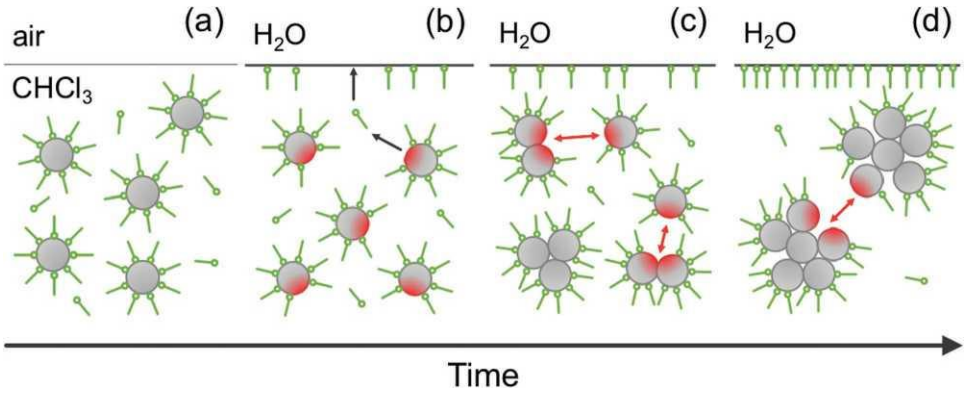

Scheme 1. Schematic representation of the process for NP assembly by CSD at a liquid-liquid interface; a) stable NP suspension before forming the liquid-liquid interface, b) an interface is formed, free stabilizer is depleted from the organic phase by adsorption to the interface, resulting in surface activated NPs, NP*; c) clusters are formed through the interaction of NP*; d) the formation of NP*, and NPC* drives ongoing assembly. The portions on the NP* and NPC* shown in red indicate surface depleted sites. Note that it is most likely that depletion of surface-bound stabilizer leads to an overall reduction in average surface coverage. We represent the activated sites as 'vacant' only for the sake of illustration.

In this paper, we report a new approach, using a water– solvent interface as the competitive substrate (WI-CSD), which enables robust, reproducible, and scalable assembly. In WI-CSD, a layer of water is introduced over an NP suspension in chloroform generating a stable liquid–liquid interface of fixed area which acts as a competing substrate with controlled capacity, see **Scheme 1**. Hence, we show for the first time the preparation of size-selected NPCs of narrow size-polydispersity reproducibly, and at scale, using only cheap starting materials. Interestingly, as the process continues the polydispersity of the clusters improves, until it is better than that of the starting NP suspensions. This is possible because all the key process parameters and experimental conditions can be specified. Using these insights, we subsequently applied WI-CSD to prepare NPCs using different NP types. This demonstrates its potential as a colloidal process for preparing nonaqueous NPC sus- pensions formed of many NP types for applications, including i) nano-compositing, following array formation/densification and ii) biomedicine, following phase transfer of intact magnetic NPC suspensions, as investigated here.

2. Results and Discussion

2.1. Preparation, Stabilization, and Primary Characterization of Size-Controlled FeO NPC Suspensions

Monodisperse primary FeO NP dispersions in $CHCl_3$, of hydro- dynamic size (d_{hyd}) *c.* 15 nm, were prepared using previously reported methods,[18] which are derived from the surfactant-free thermal decomposition process described by Pinna et al.[19] Following synthesis in benzyl alcohol (BA) the NPs were stabilized using a controlled quantity of oleic acid (OA) surfactant molecules, corresponding to 0.75 monolayer equivalents in the final suspensión (assuming a binding footprint of 3.8 x 10^{-19} m^2,[20] and 100% monodisperse spherical NPs). It was found that the assembly experiment is very sensitive to the quantity of stabilizer used in forming the NP dispersion. The surfactant-free NP strategy enables the CSD approach by providing control over coverage, see below.

In a typical assembly experiment, 1.2 mL of the FeO NP dispersion containing «2 x 10^{-3} M of Fe (at 0.75 monolayer equivalents) was placed in a standard UV cuvette. Under these conditions the suspension is stable; d_{hyd} remains unchanged at 15 nm over many days. A layer of de-ionized water, typically 0.6 mL, was carefully placed over the $CHCl_3$ suspension using a pipette. This resulted in the controlled assembly of NPCs of narrow size-polydispersity in the $CHCl_3$ suspension by gradual aggregation of NPs, as observed by continuously monitoring the suspensions using dynamic light scattering (DLS), **Figure 1**. A gradual increase in the d_{hyd} value was observed over a period of hours, and interestingly, the poly- dispersity index (PDI), gradually decreased during this time. Note that for a typical assembly reaction the dispersed NPC yield was shown by inductively coupled plasma-atomic emission spectroscopy (ICP-AES) to be *c.* 95% of the starting NP content.

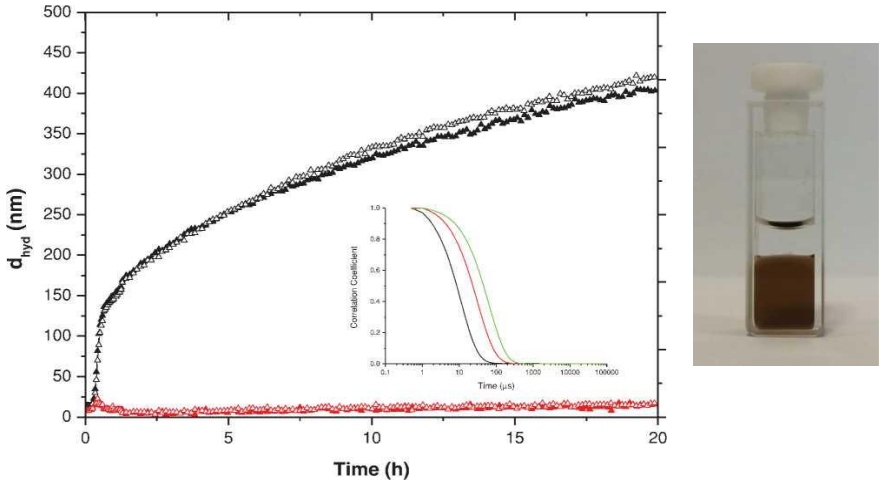

Figure 1. Left: DLS data for repeat assembly experiments forming magnetic NPCs from OA stabilized FeO NPs in $CHCl_3$ in the presence of a $CHCl_3$/ H_2O interface; hydrodynamic size (d_{hyd}) values (black), and PDI*100 (red). The inset shows normalized DLS correlograms recorded for NPs (in black) *d*hyd = 15 nm (PDI 0.08); and NPCs of size 42 nm (0.17) in red, and of size 84 nm (0.14) in green, this confirms the quality of the DLS data and the validity of using cumulants analysis. Right; image of a FeO NPC in $CHCl_3$ suspension under a H_2O interface.

Prior to introducing the interface, the NP dispersion had a PDI of <0.08, upon addition of the layer and initiation of assembly, the PDI of the sample temporarily increased to «0.15, for the NPC size range up to «40 nm, after which it decreased gradually to «0.05. This demonstrates that the NPC size distribution late in the process is relatively narrower than that of the initial NP suspension, which is a very unusual observation. Detailed analysis of the DLS correlograms confirms the complete absence of any aggregates, and that the data conform to the cumulants model. Cluster formation is confirmed by electron microscopy analysis, see Figures S1 and S2 in the Supporting Information. Excellent agreement between the d_{hyd} values (recorded for the intact NPC suspensions) and the cluster size (when dried onto a grid) was observed for all cluster sizes studied. The absence of any dispersed NPs was also confirmed.

Figure 1 shows two different assembly experiments, for suspensions prepared from different NP syntheses (and phase transferred using the same OA equivalents), confirming that with controlled starting conditions the process can be reproduced. In fact we have demonstrated near identical kinetics for six repeats prepared from different batches of NPs, see Figure S3 in the Supporting Information. Reproducibility of assembly kinetics demonstrates that the starting conditions are well defined; in this case the key parameters are a Fe concentration of 2.20 x 10^{-3} M and the use of 4.65 x 10^{-3} M of OA in the NP coupling reaction (0.75 OA monolayer equivalents). A clear specification of the initial conditions that determine kinetics of controlled particle assembly is, to the best of our knowledge, without precedent. Identifying these conditions should allow us to generalize the technique. Hence the following protocol for identifying conditions for WI-CSD (developed for OA stabilized FeO NPs in $CHCl_3$) can be applied to multiple NP types:

- Step 1: Identify if an equilibrium exists between NP-bound and free stabilizer, by serial dilution of an NP suspension. If this is the case at some concentration uncontrolled assembly (with increasing PDI) should be observed. Assuming this criterion can be met, within a useful concentration range for the application of interest, then.
- Step 2: Expose the dispersion, at a concentration where it is stable, to a liquid–liquid interface and monitor inline by DLS (e.g., at 1.2 mL scale). This fixes the dispersion volume to interface area ratio and for the selected NP concentration.
- Step 3: If unsuccessful, systematically reduce the stabilizing ligand concentration and repeat Step 2.
- Step 4: If unsuccessful, systematically lower the NP concentration and repeat Step 2.
- Step 5: If unsuccessful, systematically vary the dispersion volume to interface area ratio, then repeat Step 2.
- Step 6: Scale-up while retaining the optimized NP concentration, stabilizer content and ratio, with off-line DLS monitoring (see Section 2.4 for more details).

This method was used to demonstrate the generality of the process for 1,2-hexadecanediol-stabilized FeO and for OA stabilized TiO_2 NP suspensions, see Figure S4 in the Supporting Information. These experiments illustrate the potential of WI-CSD as a general approach to colloidal assembly of functional clusters.

2.2. The Role of the Liquid–Liquid Interface

Having established the potential of the approach and with a view to elucidating the role of the interface, a series of experiments on assembly of OA-stabilized FeO NPs was performed. First, a $CHCl_3$ NPC suspension was removed from underneath the interface using a pipette during an experiment, at a time when d_{hyd} = 67 nm (PDI 0.19) (see **Figure 2**a, arrow i). Care was taken not to disrupt the interface and a significant volume of $CHCl_3$ suspension was left behind to ensure the extracted aliquot contained no water. This aliquot was returned to the DLS instrument in a fresh cuvette and continuously monitored. It was found that the assembly rate immediately slowed, approaching zero within a few hours, Figure 2a. Subsequently a fresh aliquot of 0.6 mL water was carefully added, re-establishing a liquid–liquid interface (Figure 2a, arrow ii), restarting the assembly process with a similar rate to before. These observations demonstrate one method (removal of the interface) to arrest assembly when the preferred size has been achieved. Note that the assembly pro- cess can be rapidly stopped, and hence any NPC selected size selected, by removal of the interface and dilution of the suspension, as shown in Figure S7 in the Supporting Information. In the second experiment shown in Figure 2 an aliquot of 1.2 mL of tetrahydrofuran (THF) was added to the cuvette during an interfacial assembly experiment at time (iii), resulting in the formation of a single phase, the resulting change in viscosity caused an increase in the apparent d_{hyd} value. It was found that removing the interface in this way stopped assembly and that the resulting NPC suspension was stable; both d_{hyd} and the backscattered light intensity were unchanged for many hours. We can conclude that the presence of the liquid–liquid interface is the critical condition for the ongoing assembly process.

The solubility of OA in H_2O is known to be very low. Nevertheless, it was confirmed that the water phase itself plays no role by increasing the volume of the H_2O layer during an assembly experiment. In Figure 2b, the quantity of water was doubled from 0.6 to 1.2 mL at the time indicated, once again care was taken not to disrupt the interface. The effect on the assembly rate, which was linear with time in this case, was negligible. This confirms that any OA content in the water phase is low and does not affect cluster assembly in the organic phase and, again, that an interface is the critical condition for assembly. Finally, the effect of the NP dispersion volume on assembly is shown in Figure 2c. As the volume of $CHCl_3$ dispersion is increased the assembly rate decreases, both in the early rapid assembly stage and later during the quasi-linear stage. Our interpretation is that the rate decreases as the ratio of interfacial area (which does not change in this case) to NP concentration decreases, consistent with transfer of OA from the $CHCl_3$ suspension to the interface driving reduction in the interparticle interaction potential. In experiments described below the mechanism of assembly is more closely investigated.

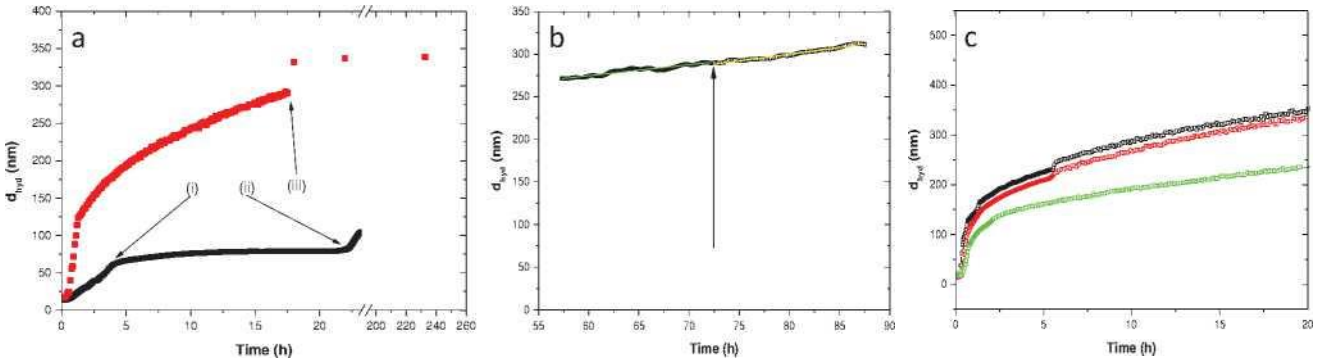

Figure 2. a) DLS data for assembly of FeO NPs in $CHCl_3$. For the experiment in black, at time i) the interface was removed, and at time ii) a fresh interface was restored over the same suspension. For the experiment in red (which was performed under different conditions, hence the difference in initial rate) at time iii) 1.2 mL of THF was added. b) The effect of increasing the volume of the H_2O layer above the $CHCl_3$ suspension during assembly; at the time indicated by the arrow the volume of the water was increased from 0.6 to 1.2 mL. The straight line is a linear fit to all the d_{hyd} values; with a slope of 1.30 ± 0.04 nm h^{-1}. c) The effect of increasing the volume of the FeO NP $CHCl_3$ suspension used in the assembly process (keeping all other parameters constant); 1.2 (black), 1.8 (red), and 2.4 mL (green), at Fe = 2.2×10^{-3} M. The occasional kinks in the data, e.g., at 5.5 h for the upper traces are DLS artifacts, see the Experimental Section.

2.3. Kinetics of Assembly by WI-CSD

The results presented in **Figure 3**a,b show the effect of free OA and NP concentration in the $CHCl_3$ suspension on the assembly process, as monitored in situ by DLS. For the experiments shown in Figure 3a the quantity of free OA added to the NP suspension, prior to introducing the water layer, was increased, and the NP concentration and total volume were held constant. For the experiments shown in Figure 3b, the NP concentration was increased, and both the total volume and the surface equivalents of OA were held constant. The resulting changes to the kinetics are broadly similar; as the amount of OA (alone), or the concentration of NPs (and hence of OA) is increased, the rate of the assembly process decreases. These observations are consistent with fixed capacity of the interface for the stabilizing ligand, as expected. The early time points were successfully fitted to an exponentially increasing function; $d = d_0 + A \exp[(t - \tau_0)/\tau_a]$ where d_0 is the initial size, A an amplitude factor, τ_0 the induction time, and τ_a^{-1} the (exponential) assembly rate (see Supporting Information for more details). It can be seen that increasing the ratio of the OA to surface area of the interface (ratio in μg cm^{-2}), results in an exponential increase in τ_0, Figure 3c, and an exponential decrease in τ_a^{-1}, Figure 3d.

Our proposed mechanism for cluster assembly is that the liquid–liquid interface provides a sink for free surfactant molecules in suspension, altering the equilibrium between NP-bound and free surfactant, which generates a very low concentration of NPs partially destabilized due to depletion of surface-bound surfactant molecules, or NP*, see Scheme 1 (Note that the absence of direct NP–NP contacts in TEM analysis of the NPCs, Figure S1 in the Supporting Information, suggests that ligand depletion causes a gradual reduction in overall ligand coverage, as opposed to producing vacant sites). NP* then collide with other NP* with a higher probability of binding, due to reduced steric contributions to the interparticle interaction potential, to form NPCs, as reported in more detail in previous work.[17] As the process continues, NPCs are themselves subject to ongoing stabilizer desorption, but the smaller clusters within the size distribution are more active due to their larger surface area and faster diffusion which increases the probability of successful collisions. Hence the relative monodispersity of the size distribution improves, which is a defining characteristic of CSD and is reminiscent of the size focusing process in NP synthesis.[21] Detailed kinetic modeling requires simulation of interparticle interactions for size distributions of finite width as a function of time using the Population Balance Equation, e.g., by the Smoluchowski aggregation approach or similar formalism,[22,23] work which is ongoing. In the interim, the observed transitions between early exponential, to later linear, assembly profiles can be interpreted in terms of the highest probability collisions in the evolving population at a given stage, see Supporting Information (Figure S5, Supporting Information) for more detailed discussion

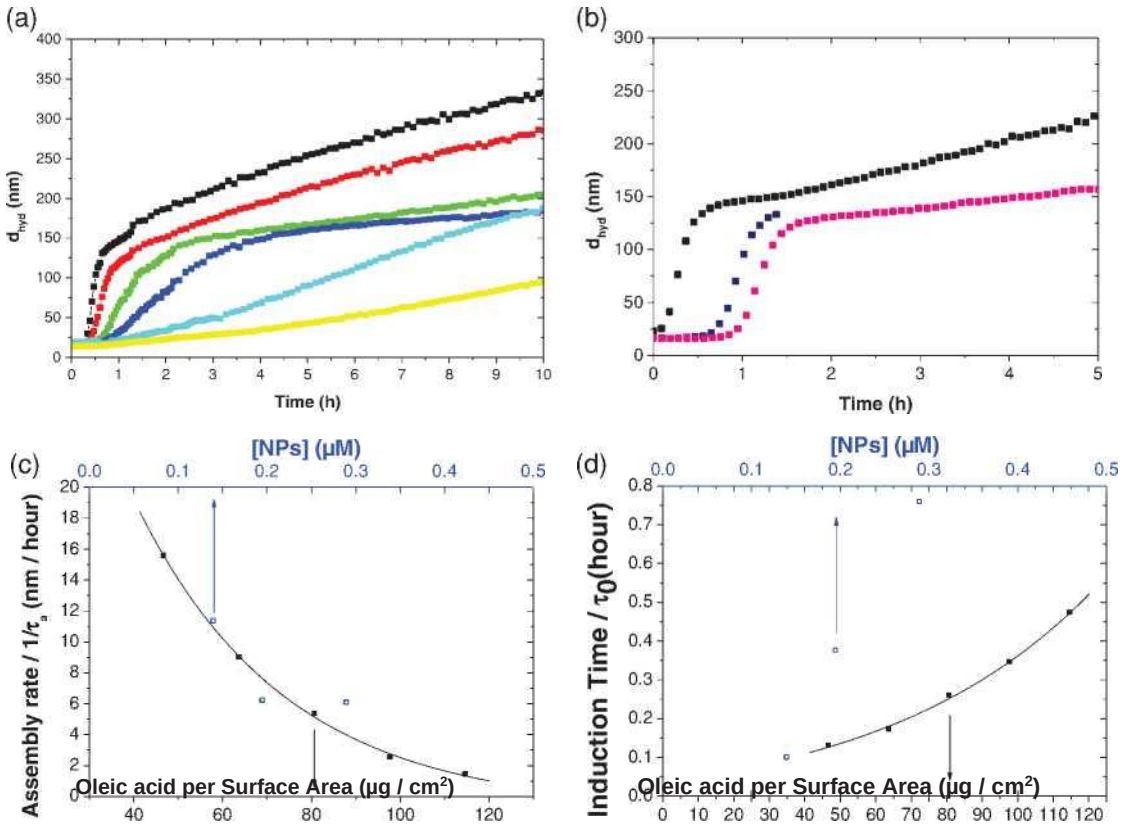

Figure 3. a) Kinetics of particle assembly for suspensions with 0 (■), 25 (■), 50 (■), 75 (■), 100 (■), and 125 Jlg (□)OA added to the 1.2 mL $CHCl_3$ NP dispersion. All suspensions were initially phase transferred with 0.75 surface equivalents of OA, and the Fe concentration was 2.2 X 10^{-3} M or 0.39 X 10^{-6} M NPs. b) Kinetics of particle assembly for suspensions phase transferred with 0.75 surface equivalents (see the text) of OA with Fe concentration of 0.140 (■), 0.195 (■), and 0.290 (■) X 10^{-3} M. The early stage data for the profiles were successfully fitted to a single exponential. For the eight experiments shown in a) and b) the effect of the OA/surface area ratio (■), and NP concentration (□), on the induction time, τ_o, is shown in c), and on the exponential assembly rate, τ_a^{-1}, in d).

2.4. Scaling-Up the WI-CSD Process

Having identified and optimized the key process parameters that determine assembly, i.e., the surface excess of OA dispersion, volume to interface area ratio, and NP concentration, we found that by fixing these parameters it is possible to scale-up the process. The results presented in **Figure 4** demonstrate successful scale-up of assembly from 1.2 to 60, and then to 150 mL, i.e., by a factor of 125, which was achieved by keeping these three parameters constant. Note that at 60 and 150 mL scale the DLS measurements were off-line, but the assembly kinetics are the same as the in-line (1.2 mL) experiment, with comparably good monodispersity (PDI < 0.1) and while maintaining excellent yield (*c.* 95%, as measured by ICP-AES). Hence the batch process can be scaled up by two orders of magnitude while maintaining the excellent product yield with almost iden- tical kinetics, using a dispersion volume to surface area ratio of 1.2:1 (mL NP dispersion:cm^2 surface area) in each case. At 150 mL scale, it is necessary to physically stabilize the interface using a mesh scaffold which minimizes tipping of the H_2O layer, see Figure 4. A further factor of 10 in scale could be easily achieved with an array of 10 X 150 mL flasks. Since both phases are liquid, we consider that the process has the potential for further up-scale or parallelization through modifications of the interface.

In the case of magnetic FeO NPCs, having scaled-up the pro- cess it was possible to identify suitable conditions for almost quantitative (>95%) phase transfer of magnetic FeO NPCs, using either surfactants or block co-polymers, to form stable aqueous NPC suspensions without significant change in d_{hyd}, or loss of monodispersity, see Figure S6 in the Supporting Information, so retaining the key advantages of CSD.

3. Conclusions

In summary, in the WI-CSD approach to colloidal assembly of NPs, the assembly rate can be readily modified through control over experimental parameters, and in particular the ligand to surface area ratio. The sensitivity of the process to the initial state makes it possible to identify conditions, for different NP and ligand types, under which assembly can be controlled (clusters of increasing monodispersity can be prepared and the process stopped at the desired size). The approach can be scaled-up by a factor of more than 100 while retaining size control, monodispersity, and the kinetics of assembly. Hence we have demonstrated that WI-CSD is a robust, cheap, generally applicable process for reproducibly preparing stable NP clusters of narrow size-polydispersity (better than that of the initial stable NP suspensions). In

particular, as the process been demonstrated using nonpolar[14,15] and now polar organic solvents, it may be possible to identify suitable condition for aqueous suspensions; that work is ongoing. WI-CSD provides insights into how interparticle interactions can be controlled through application of eternal stimuli, to drive cluster formation with retention of monodispersity, with the colloidal remaining close to equilibrium throughout. We note potential applications of magnetic NPCs in biomedicine, indeed the possibility to determine magnetic resonance properties using CSD through independent control of NP and NPC size has been described,[17] in addition TiO_2 NPCs may be applied in light harvesting, although many others may be possible given the generality of the approach.

4. Experimental Section

Synthesis: Stable $CHCl_3$ suspensions of primary maghemite NPs were prepared using methods previously reported,[16] derived from the process described by Pinna et al.[19] Iron (III) acetylacetonate, Fe(III)(acac)$_3$ (purity >99.9%), OA (>99.0%), and BA (>99.0%) were purchased from Sigma- Aldrich. All reagents were used without further purification. Reagent grade chloroform was purchased from Labscan and dried over freshly regenerated molecular sieves. De-ionized water was obtained from a Millipore MilliQ system and had a resistance of >16 mQ prior to use. In a typical synthesis 1.00 g (2.832 mmol) of Fe(III)(acac)$_3$ and 20 mL (0.193 mol) of BA was transferred to a three neck round bottom flask equipped with a nitrogen flow system, a condenser, and a thermometer. The mixture was de-oxygenated at room temperature by N_2 purging for 15 min. A nitrogen atmosphere was maintained for the duration of the reaction. In all cases, the reaction reached reflux at =195 °C within 15 min. The reaction refluxed for 7 h without stirring and during the reaction, a colour change from red to black was observed. The FeO concentration was determined gravimetrically and was typically =10.5 mg mL^{-1}.[24]

Titanium dioxide NPs were prepared following the protocol described in the previous paragraph. In this case, 1.41 mL (4.762 mmol) of titanium (IV) isopropoxide, purchased also from Sigma-Aldrich (purity >97.0%), was added to a three neck round bottom flask containing 20 mL (0.193 mol) of BA. The reaction was refluxed for 7 h. During the reaction the mixture turned from a clear solution to a milky slurry. For TiO_2 NP synthesis, the typical NP concentration was =23.5 mg mL^{-1}, as determined gravimetrically.

Stabilization: 1.5 mL of concentrated FeO NP suspension was precipitated out using centrifugation and washed twice with $CHCl_3$. For each ligand (OA and 1,2-hexadecanediol), typically 0.10–0.18 mL of a 10 mg mL^{-1} ligand solution was added to the coarse product. This is equivalent to a 0.75-fold equivalent of the ligand needed to form a monolayer on the surface of the NPs (assuming spherical NP with a core size obtained from TEM of 8.2 nm and a footprint of 38.0 $Å^2$ for OA and a footprint of 17.3 $Å^2$ for 1,2-hexadecanediol). This mixture was shaken using a vortex mixer and the final volume was made up to 1.5 mL using $CHCl_3$. The dispersion was shaken overnight to allow for the complete surface coating of the NPs. The stabilized NPs were centrifuged for 10 min at 13 200 rpm in order to remove aggregates, resulting in a dark brown stabilized NP suspension, typically of about 140 X 10^{-3} M (Fe concentration) which was stable for many months, as measured by DLS.

To stabilize the TiO_2 NPs (assuming spherical NP with a core size about 10.0 nm obtained from TEM), with OA (footprint of 38.0 $Å^2$), the same protocol was followed described above, adding around 0.40 mL of ligand to form a monolayer on the surface.

Assembly: For the assembly stage, 50 ^L of the concentrated stabilized NP solution and 1.4 mL of $CHCl_3$ was centrifuged for 10 min at 13 200 rpm in order to remove any aggregates present, thereafter the precipitate was discarded. From this, 1.2 mL of the centrifuged solution was placed in a standard 1 cm^2 glass/quartz cuvette and its size was analysed by DLS using a Malvern NanoZS. Typically at this point the suspension had a concentration of = 2.2 X 10^{-3} M [Fe]. To initiate assembly, 0.6 mL of de-ionized water was placed carefully over the solution, ensuring the water formed a uniform layer with a clear interface boundary.

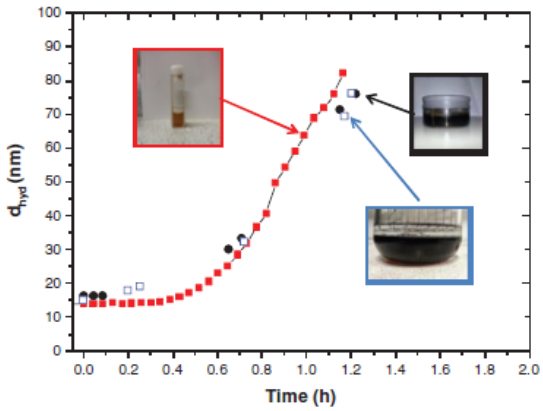

Figure 4. DLS data demonstrating the effect of scale-up of the assembly process for FeO NPs in $CHCl_3$ placed under a water layer, at 1.2 mL ($CHCl_3$ volume) scale (■) and monitored in-line, also at 60 mL (●), and at 150 mL scale (□), both monitored off-line. Fe concentration =2.2 X 10^{-3} M, OA concentration of = 1.85 X 10^{-9} M and volume to area ratio of 1.2: 1.

DLS: DLS experiments were performed at 25 °C on a Malvern NanoZS (Malvern Instruments, Malvern UK) which uses a detection angle of 173°, and a 3 mW He-Ne laser operating at a wavelength of 633 nm. The Z-Average (mean hydrodynamic) diameter, which was referred to as d_{hyd}, and the PDI values were obtained from analysis of the correlation functions using the Multiple Narrow Modes algorithm based upon a nonnegative least-squares fit using Dispersion Technology software (v. 4.10, Malvern Instruments; Worcestershire, U.K.). Note that minor shifts in d_{hyd} and the count rate could occur when the measurement parameters (attenuator index, cuvette position) of the DLS instrument were adjusted to optimize the data acquisition, see Figure 2c.

Electron Microscopy: All TEM images were obtained using a JEOL 2000 FX TEM scan (at an accelerating voltage of 80 kV) for samples deposited on carbon-coated (400 mesh) copper grids. The preparation of samples for TEM analysis involved depositing a drop (15 gL) onto the grids and allowing the solvent to evaporate, prior to imaging. STEM images were obtained using a Hitachi S5500 Field-Emission SEM (at an accelerating voltage of 20 kV) and prepared as described above.

Acknowledgements

The research leading to these results has received funding from Science Foundation Ireland (under the projects 15/TIDA/2945 and 16/IA/4584). The authors would like to thank Dr. Brendan Twamley for assistance with scanning electron microscopy. The authors also thank Dr. Tiina O'Neill, Conway Institute, University College Dublin, for access and assistance with TEM.

References

[1] J.-H. Lee, Y.-M. Huh, Y.-W. Jun, J.-W. Seo, J.-T. Jang, H.-T. Song, S. Kim, E.-J. Cho, H.-G. Yoon, J.-S. Suh, J. Cheon, *Nat. Med.* **2007**, *13*, 95.
[2] Y.-M. Huh, Y.-W. Jun, H.-T. Song, S. Kim, J.-S. Choi, J.-H. Lee, S. Yoon, K.-S. Kim, J.-S. Shin, J.-S. Suh, J. Cheon, *J. Am. Chem. Soc.* **2005**, *127*, 12387.
[3] J. Xie, J. Huang, X. Li, S. Sun, X. Chen, *Curr. Med. Chem.* **2009**, *16*, 1278.
[4] B. P. Barnett, A. Arepally, P. V. Karmarkar, D. Qian, W. D. Gilson, P. Walczak, V. Howland, L. Lawler, C. Lauzon, M. Stuber, D. L. Kraitchman, J. W. M. Bulte, *Nat. Med.* **2007**, *13*, 986.
[5] L. Lartigue, P. Hugounenq, D. Alloyeau, S. P. Clarke, M. Lévy, J.-C. Bacri, R. Bazzi, D. F. Brougham, C. Wilhelm, F. Gazeau, *ACS Nano* **2012**, *6*, 10935.
[6] J. K. Stolarczyk, A. Deak, D. F. Brougham, *Adv. Mater.* **2016**, *28*, 5400.
[7] R. B. Grubbs, *Nat. Mater.* **2007**, *6*, 553.
[8] N. C. Bigall, A. Curcio, M. P. Leal, A. Falqui, D. Palumberi, R. Di Corato, E. Albanesi, R. Cingolani, T. Pellegrino, *Adv. Mater.* **2011**, *23*, 5645.
[9] U. I. Tromsdorf, N. C. Bigall, M. G. Kaul, O. T. Bruns, M. S. Nikolic, B. Mollwitz, R. A. Sperling, R. Reimer, H. Hohenberg, W. J. Parak, S. Förster, U. Beisiegel, G. Adam, H. Weller, *Nano Lett.* **2007**, *7*, 2422.
[10] J. Fresnais, C. Lavelle, J. F. Berret, *J. Phys. Chem. C* **2009**, *113*, 16371.
[11] A. Sánchez-Iglesias, M. Grzelczak, T. Altantzis, B. Goris, J. Pérez-Juste, S. Bals, G. Van Tendeloo, S. H. Donaldson, B. F. Chmelka, J. N. Israelachvili, L. M. Liz-Marzán, *ACS Nano* **2012**, *6*, 11059.
[12] J. Zhuang, H. Wu, Y. Yang, Y. C. Cao, *J. Am. Chem. Soc.* **2007**, *129*, 14166.
[13] E. L. Rosen, R. Buonsanti, A. Llordes, A. M. Sawvel, D. J. Milliron, B. A. Helms, *Angew. Chem., Int. Ed.* **2012**, *51*, 684.
[14] J. K. Stolarczyk, S. Ghosh, D. F. Brougham, *Angew. Chem., Int. Ed.* **2009**, *48*, 175.
[15] C. J. Meledandri, J. K. Stolarczyk, D. F. Brougham, *ACS Nano* **2011**, *5*, 1747.
[16] T. Ninjbadgar, E. K. Fox, J. Hierrezuelo, F. El Haddassi, D. F. Brougham, *J. Mater. Chem. B* **2015**, *3*, 8638.
[17] J. K. Stolarczyk, C. J. Meledandri, S. P. Clarke, D. F. Brougham, *Chem. Commun.* **2016**, *52*, 13337.
[18] T. Ninjbadgar, D. F. Brougham, *Adv. Funct. Mater.* **2011**, *21*, 4769.
[19] N. Pinna, S. Grancharov, P. Beato, P. Bonville, M. Antonietti, M. Niederberger, *Chem. Mater.* **2005**, *17*, 3044.
[20] A. Wooding, M. Kilner, D. B. Lambrick, *J. Colloid Interface Sci.* **1991**, *144*, 236.
[21] X. Peng, J. Wickham, A. P. Alivisatos, *J. Am. Chem. Soc.* **1998**, *120*, 5343.
[22] M. Smoluchowski, *Z. Phys. Chem.* **1917**, *92*, 129.
[23] N. Fuchs, *Z. Phys.* **1934**, *89*, 736.
[24] C. J. Meledandri, J. K. Stolarczyk, S. Ghosh, D. F. Brougham, *Lang- muir* **2008**, *24*, 14159.